

# RSC Advances



This is an *Accepted Manuscript*, which has been through the Royal Society of Chemistry peer review process and has been accepted for publication.

*Accepted Manuscripts* are published online shortly after acceptance, before technical editing, formatting and proof reading. Using this free service, authors can make their results available to the community, in citable form, before we publish the edited article. This *Accepted Manuscript* will be replaced by the edited, formatted and paginated article as soon as this is available.

You can find more information about *Accepted Manuscripts* in the [Information for Authors](#).

Please note that technical editing may introduce minor changes to the text and/or graphics, which may alter content. The journal's standard [Terms & Conditions](#) and the [Ethical guidelines](#) still apply. In no event shall the Royal Society of Chemistry be held responsible for any errors or omissions in this *Accepted Manuscript* or any consequences arising from the use of any information it contains.

Cite this: DOI: 10.1039/c0xx00000x

www.rsc.org/xxxxxx

ARTICLE TYPE

# Towards applications in catalysis: Investigation on photocatalytic activities of a derivative family of the Keplerate type molybdenum-oxide based polyoxometalates

Yunshan Zhou,\* Libo Qin, Chao Yu, Tian Xiong, Lijuan Zhang,\* Waqar Ahmad, and Hao Han

Received (in XXX, XXX) Xth XXXXXXXXX 20XX, Accepted Xth XXXXXXXXX 20XX  
DOI: 10.1039/b000000x

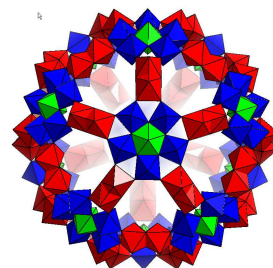
The photocatalytic potential of a derivative family of the Keplerate type nano-porous Mo-O based polyoxometalates with general formula  $[\text{Mo}^{\text{VI}}_{72}\text{Mo}^{\text{V}}_{60}\text{O}_{372}(\text{L})_{30}(\text{H}_2\text{O})_{72}]^{n-}$  ( $\text{L} = \text{CH}_3\text{COO}^-$ ,  $\text{SO}_4^{2-}$ ) (denoted  $\text{Mo}_{132}$ ) has been evaluated by a prototype photocatalytic decoloration reaction of aqueous rhodamine B. The  $\text{Mo}_{132}$  anions are found to be photocatalytically active centers, however they are unstable and subjected to decompose in solution form. The introduction of organic counter cations such as tetrabutylammonium ( $n\text{-Bu}_4\text{N}^+$ ) and dioctadecyldimethylammonium ( $\text{DODA}^+$ ) can endow significant stability to the giant anions during the catalytic process. TOC changes and GC/MS measurements were done to identify the degradation products. Among the derivatives, the compound **2** composed of  $n\text{-Bu}_4\text{N}^+$  and  $\text{Mo}_{132}$  ( $\text{L} = \text{CH}_3\text{COO}^-$ ) has been found the most active one towards the photocatalytic decoloration of RhB solution. Analytical mechanism indicates that both  $\cdot\text{OH}$  radicals and  $^1\text{O}_2$  participate in the photo degradation process.

## Introduction

Polyoxometalates (POMs) constitute an enormous class of inorganic clusters, which can be characterized by a fascinating variety of architectures, topologies and excellent physicochemical properties including strong Brønsted acidity, high proton mobility, fast multi-electron transfer, high solubility in various solvents and resistance to the hydrolytic and oxidative degradations in solutions.<sup>1-2</sup> Bearing in mind that increasing the size and complexity of POMs can generate variable functionality of interest, the unique nano-sized porous POMs of Keplerate type with general formula  $[\text{Mo}^{\text{VI}}_{72}\text{Mo}^{\text{V}}_{60}\text{O}_{372}(\text{L})_{30}(\text{H}_2\text{O})_{72}]^{n-}$  ( $\text{L} = \text{CH}_3\text{COO}^-$ ,  $\text{SO}_4^{2-}$ ,  $\text{HCOO}^-$ , et al) (denoted  $\text{Mo}_{132}$ , Scheme 1) have been designed and synthesized by Müller's group.<sup>3-4</sup> The Keplerates are composed of 72  $\text{Mo}^{\text{VI}}$  and 60  $\text{Mo}^{\text{V}}$ , that constitute a capsule of 2.9 nm, 20  $\{\text{Mo}_9\text{O}_9\}$  pores and a cavity connected outside *via* 20 channels, these inner shell can be modified by various ligands such as  $\text{CH}_3\text{COO}^-$ ,  $\text{HPO}_4^{2-}$ ,  $\text{PO}_4^{3-}$  and  $\text{SO}_4^{2-}$ , which correspond to different anionic and cationic charges for charge balance. So far, a variety of applications for such unique POMs have been found in the fields like nano-separation chemistry,<sup>5</sup> cell simulation,<sup>6</sup> materials,<sup>7-8</sup> magnetic,<sup>9</sup> optical properties,<sup>10</sup> water decontamination,<sup>11</sup> environment related carbon dioxide picking and so on.<sup>12</sup>

On the other hand, it is well known that polyoxometalates have been widely used as acids, reductant-oxidants, photochemical or electrochemical catalysts for industrial organic reactions<sup>13-14</sup> because of their easily adjustable catalytic properties, high thermal stability, non-toxicity and environment friendly

characters. Being new members of polyoxometalates, the Keplerate type POMs have also been expected as catalysts. Indeed, interesting catalytic activities like reversible cleavage and methyl tert-butyl ether synthesis,<sup>15</sup> regioselective Huisgen reactions,<sup>16</sup> and selective oxidation of sulfides under confined conditions<sup>17</sup> have already been reported. However, so far photocatalytic behaviour of the Keplerate type POMs, which is expected very interesting and important in both theoretical and practical view, still remains unexplored.



**Scheme 1.** Polyhedral representation of the structure of the anion  $[\text{Mo}^{\text{VI}}_{72}\text{Mo}^{\text{V}}_{60}\text{O}_{372}(\text{L})_{30}(\text{H}_2\text{O})_{72}]^{n-}$  ( $\text{L} = \text{CH}_3\text{COO}^-$ ,  $\text{SO}_4^{2-}$ ,  $\text{HCOO}^-$ , .....).  $\text{Mo}(\text{VI})$  atoms are shown in blue and green, and  $\text{Mo}(\text{V})$  atoms in red.

In this paper, the photocatalytic potential of the nano-porous Keplerates type POMs, namely,  $(\text{NH}_4)_{42}[\text{Mo}^{\text{VI}}_{72}\text{Mo}^{\text{V}}_{60}\text{O}_{372}(\text{CH}_3\text{COO})_{30}(\text{H}_2\text{O})_{72}] \cdot ca.300\text{H}_2\text{O} \cdot ca.10\text{CH}_3\text{COONH}_4$  **1**<sup>3</sup>,  $(\text{NH}_4)_{18}(n\text{-Bu}_4\text{N})_{24}[\text{Mo}^{\text{VI}}_{72}\text{Mo}^{\text{V}}_{60}\text{O}_{372}(\text{H}_2\text{O})_{72}(\text{CH}_3\text{COO})_{30}] \cdot ca.7\text{CH}_3\text{COONH}_4 \cdot ca.173\text{H}_2\text{O}$  **2**<sup>18</sup>,  $(\text{NH}_4)_{72}[\text{Mo}^{\text{VI}}_{72}\text{Mo}^{\text{V}}_{60}\text{O}_{372}(\text{SO}_4)_{30}(\text{H}_2\text{O})_{72}] \cdot ca.200\text{H}_2\text{O}$  **3**<sup>4</sup>,  $(\text{NH}_4)_{44}(n\text{-Bu}_4\text{N})_{28}[\text{Mo}^{\text{VI}}_{72}\text{Mo}^{\text{V}}_{60}\text{O}_{372}(\text{SO}_4)_{30}(\text{H}_2\text{O})_{72}] \cdot ca.210\text{H}_2\text{O}$

4 and  
 (DODA)<sub>40</sub>(NH<sub>4</sub>)<sub>2</sub>[Mo<sup>VI</sup><sub>72</sub>Mo<sup>V</sup><sub>60</sub>O<sub>372</sub>(CH<sub>3</sub>COO)<sub>30</sub>(H<sub>2</sub>O)<sub>72</sub>]·ca.50H<sub>2</sub>O **5**<sup>8</sup>, were investigated *via* degradation of rhodamine B(RhB) solution (difficult to degrade completely by conventional  
 5 methods and also suspected to be carcinogenic), which is often used as a prototype to examine the catalytic behavior of a photocatalyst.

## Experimental

### Materials and instruments

10 All chemicals and reagents were of analytical grade and used without further purification. Commercially available photocatalyst TiO<sub>2</sub> (Aladdin reagent, EP grade, average size 0.2 ~ 0.4 μm) was used as received. IR spectra were recorded on a MAGNA-IR 750 (Nicolet) spectrophotometer with KBr pellets in  
 15 400 ~ 4000 cm<sup>-1</sup> region. Thermogravimetric analyses were carried out on a NETZSCH STA 449C unit at a heating rate of 5°C/min under air atmosphere. Elemental analyses for C, H and N were performed on a Perkin-Elmer 240C analytical instrument, Analyses for Mo were performed by the SPECTRO ARCOS type  
 20 inductively coupled plasma spectrometer. UV-vis absorption spectra were recorded on a SHIMADZU UV-2550 spectrometer. GC/MS analyses were carried out on a Shimadzu GC/MS-QP2010 instrument equipped with a DB-5MS capillary column (30 m × 0.25 mm). The temperature program of the column was  
 25 set as follows: at 60°C, hold time =1 min; from 60 to 250 °C, rate 20 °C/min. The samples for GC/MS analyses were prepared as follows: After the catalyst were removed by centrifugation, the remained aqueous solution was collected and evaporated to near dryness under reduced pressure; methanol (10 ml each time) was  
 30 added and evaporated three times to remove water completely; finally, the remaining residue was dissolved in 0.5 ml of methanol. TOC determination of the samples (filtered through polycarbonate membranes with an average pore diameter of 15 nm) was performed on a Shimadzu TOC-5000A analyzer.  
 35 Photoluminescence spectra were recorded on a Hitachi F-7000 fluorescence spectrophotometer with emission slit of 5 nm by using a 150W xenon lamp as the light source. ICP analysis for Mo were conducted on a Spectro Arcos Eop Axial View Inductively Coupled Plasma Spectrometer.

40 During catalytic reaction processes, all illumination process was performed using a BYLAB UV-III UV light desktop equipped with a 12 W lamp (light intensity 13 μW/cm<sup>2</sup>) of irradiation wavelength 365 nm, except one experiment where a 250-W mercury lamp (light intensity 22 mW/cm<sup>2</sup>) was employed  
 45 as a light source to test the influence of light intensity on the degradation effect. The light intensity was measured by a radiometer (FZ-A, Photoelectric instrument factory of Beijing Normal University, China).

### Synthesis of the compounds

50 (NH<sub>4</sub>)<sub>42</sub>[Mo<sup>VI</sup><sub>72</sub>Mo<sup>V</sup><sub>60</sub>O<sub>372</sub>(CH<sub>3</sub>COO)<sub>30</sub>(H<sub>2</sub>O)<sub>72</sub>]·ca.300H<sub>2</sub>O·ca.10 CH<sub>3</sub>COONH<sub>4</sub> (compound **1**) was synthesized as described in literature.<sup>3</sup> Elemental analysis (%) calcd: C 3.36, H 3.78, N 2.55, Mo 44.25; Found: C 3.45, H 3.69, N 2.63, Mo 43.96. IR (ν/cm<sup>-1</sup>, KBr): 3424(m), 3170(m), 2958(w, (ν<sub>as</sub>(C-H))), 2862(w, ν<sub>s</sub>(C-H)),  
 55 1622 (m, ν(H<sub>2</sub>O)), 1546(m, ν(COO<sup>-</sup>)), 1441(sh), 1403(m, ν<sub>s</sub>(COO<sup>-</sup>), ν<sub>as</sub>(NH<sub>4</sub><sup>+</sup>)), 969(m), 934(w-m, Mo=O), 855(m), 792(s),

723(s), 629(w), 568(s) (Figure S1).

(NH<sub>4</sub>)<sub>18</sub>(*n*-Bu<sub>4</sub>N)<sub>24</sub>[Mo<sup>VI</sup><sub>72</sub>Mo<sup>V</sup><sub>60</sub>O<sub>372</sub>(CH<sub>3</sub>COO)<sub>30</sub>(H<sub>2</sub>O)<sub>72</sub>]·ca.7CH<sub>3</sub>COONH<sub>4</sub>·ca.173H<sub>2</sub>O (compound **2**) was prepared as described in literature.<sup>18</sup> Elemental analysis (%) calcd: C 17.61, H 4.27, N 2.20, Mo 40.53; Found: C 17.41, H 4.20, N 2.23, Mo 40.62. IR (ν/cm<sup>-1</sup>, KBr): 3430(m), 3173(m), 2968(m, ν<sub>as</sub>(C-H)), 2870(m, ν<sub>s</sub>(C-H)), 1623(m, ν(H<sub>2</sub>O)), 1557(m, ν(COO<sup>-</sup>)), 1440(sh),  
 65 1404(m, ν<sub>s</sub>(COO<sup>-</sup>), ν<sub>as</sub>(NH<sub>4</sub><sup>+</sup>)), 978(m), 951(w-m)(Mo=O), 855(m), 801(s), 732(s), 633(w), 576(s)) (Figure S1).

(NH<sub>4</sub>)<sub>72</sub>[Mo<sup>VI</sup><sub>72</sub>Mo<sup>V</sup><sub>60</sub>O<sub>372</sub>(SO<sub>4</sub>)<sub>30</sub>(H<sub>2</sub>O)<sub>72</sub>]·ca.200H<sub>2</sub>O (compound **3**) was synthesized as described in literature.<sup>4</sup> Elemental analysis (%) calcd: H 3.03, N 3.64, Mo 45.72; found: H 2.96, N 3.54, Mo 45.64. IR (ν/cm<sup>-1</sup>, KBr): 3418(s), 3172(s), 1629(m, ν(H<sub>2</sub>O)), 1440(sh), 1401(m, ν<sub>as</sub>(NH<sub>4</sub><sup>+</sup>)), 1185(w), 1134(w), 1041(w, ν<sub>as</sub>(SO<sub>4</sub><sup>2-</sup>)), 966(m), 849(m), 795(s), 720(s), 630(w), 567(s) (Figure S2).

(NH<sub>4</sub>)<sub>44</sub>(*n*-Bu<sub>4</sub>N)<sub>28</sub>[Mo<sup>VI</sup><sub>72</sub>Mo<sup>V</sup><sub>60</sub>O<sub>372</sub>(SO<sub>4</sub>)<sub>30</sub>(H<sub>2</sub>O)<sub>72</sub>]·ca.210H<sub>2</sub>O (compound **4**) was prepared with the following procedure: A 15 ml aqueous solution of compound **3** (0.25 g) and a 15 ml aqueous solution of *n*-Bu<sub>4</sub>NBr (0.23 g) (molar ratio compound **3** : *n*-Bu<sub>4</sub>NBr = 1 : 72), both having pH of ca. 3 adjusted by using  
 80 dilute CH<sub>3</sub>COOH (30%), respectively, were mixed together under fast stirring. After 20 min. of stirring, the resulting brown precipitates were filtered, washed with de-ionized water till negative AgNO<sub>3</sub> test and dried in air. Elemental analysis (%) calcd: C 15.75, H 5.15, N 2.95, Mo 37.07; Found: C 15.78, H  
 85 4.28, N 2.81, Mo 37.15; IR (ν/cm<sup>-1</sup>, KBr): 3418(s), 3172(s), 2968(ν<sub>as</sub>(C-H)), 2878(ν<sub>s</sub>(C-H)), 1641(m, ν(H<sub>2</sub>O)), 1461(w), 1407(m, ν(NH<sub>4</sub><sup>+</sup>)), 1166(w), 1119(w), 1056 (w, ν<sub>as</sub>(SO<sub>4</sub><sup>2-</sup>)), 972(m), 855(m), 792(s), 729(s), 633(w), 570(s) (Figure S2).

(DODA)<sub>40</sub>(NH<sub>4</sub>)<sub>2</sub>[Mo<sup>VI</sup><sub>72</sub>Mo<sup>V</sup><sub>60</sub>O<sub>372</sub>(CH<sub>3</sub>COO)<sub>30</sub>(H<sub>2</sub>O)<sub>72</sub>]·ca.5  
 90 0H<sub>2</sub>O (compound **5**) was prepared according to the reference.<sup>8</sup> Elemental analysis (%) calcd: C 42.49, H 7.99, N 1.32, Mo 28.35; Found: C 42.55, H 7.89, N 1.23, Mo 28.42; IR (ν/cm<sup>-1</sup>, KBr): 3436(s), 2932(ν<sub>as</sub>(C-H)), 2860(ν<sub>s</sub>(C-H)), 1659(m, ν(H<sub>2</sub>O)), 1548(m, ν(COO<sup>-</sup>)), 1467(w), 1410(m, ν(NH<sub>4</sub><sup>+</sup>), ν<sub>s</sub>(COO<sup>-</sup>)),  
 95 978(m), 951(sh), 852(m), 801(s), 732(s), 630(w), 573(s) (Figure S3).

The TG-DTA curve (Figure S4) and thermogravimetric analysis for compound **4** are given in the supporting information part.

### 100 Catalytic reaction

RhB was dissolved in deionized water to get a 2.0~6.0 mg/L solution and the desired pH was adjusted with dilute acetic acid or ammonia. Compounds **2**, **4** and **5** were grinded by using agate mortar. To 50 ml RhB solution with desired concentration in a  
 105 100 ml beaker, compounds **1** ~ **5** of desired amount were added under stirring, respectively. Dark treatments with 15 mins were done to avoid the effect of adsorption of the dye before all the measurement. Reaction samples were taken at regular intervals to analyze the absorbance change of RhB (λ<sub>max</sub>= 554 nm) using a  
 110 UV-vis spectrophotometer.

Absorbance and RhB concentration were governed by the Lambert-Beer law: A = log (I<sub>0</sub>/I) = ε·c·l, where A: absorbance (measured in 1 cm quartz cells, cm<sup>-1</sup>); I<sub>0</sub>, I: intensity of light entering and leaving the optical cell, respectively; ε: extinction

coefficient or absorptivity ( $L \cdot \text{mg}^{-1} \cdot \text{cm}^{-1}$ );  $l$ : optical path length (cm);  $c$ : concentration of dye ( $\text{mg}/l$ ). The absorbance change of RhB ( $\lambda_{\text{max}} = 554 \text{ nm}$ ) was corresponded to the concentration changes of RhB, so the decoloration ratio (DC) was calculated by the equation:  $\text{DC} = [(A_0 - A_t)/A_0] \times 100 \%$ , where  $A_0$  represents the absorbance before reaction, and  $A_t$  the absorbance at a given time.

## Results and discussion

### Factors influencing the photocatalytic effect

In the preliminary experiments, the compound **2** was used as a catalyst and it was found that RhB was remarkably degraded under UV irradiation as compare to other conditions (see Table 1). The results showed that UV irradiation and catalyst are compulsory for the degradation of RhB.

**Table 1** Preliminary RhB degradation results under various conditions<sup>[a]</sup>

Batch	Compound <b>2</b>	UV light	Sunlight	Reaction time (h)	Decoloration ratio (%)
No.1	×	×	✓	6	1.5
No.2	×	✓	×	6	3.1
No.3	✓	×	✓	6	52.7
No.4	✓	✓	×	6	92.2
No.5	✓	×	×	6	1.3

[a] Symbols ✓ and × mean that the item is present and absent, respectively. Reaction condition: 2.0 mg of compound **2**, 50 ml of 2 mg/L RhB solution and pH = ca. 5.1.

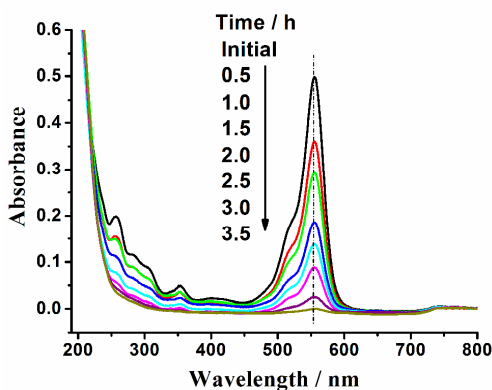


**Fig. 1.** UV-vis absorption spectral changes of RhB during the catalytic process (The arrow marks the increase of reaction time). Reaction condition: pH 3.5, 2.0 mg of compound **2** and 50 ml of 2 mg/L RhB solution.

Effect of pH on photocatalytic decolorizing efficiency using compound **2** has been done and the RhB solution was completely decolorized with decoloration ratio of almost 100% under optimized conditions (pH 3 ~ 5) (Table 2). The experimental results strengthened the fact that acidic condition is favorable for the degradation of RhB molecules as the cases for other polyoxometalates.<sup>19</sup> However, at very low pH, brown colour was observed in the system indicating the dissolution of compound **2**, which leads to easy decomposition of the anion, while very high pH the compound **2** is also apt to directly decompose.

The light intensity has significant influence on the decoloration

results, as almost 100% decoloration ratio was observed within 75 min (Table 2, Figure 2) by using 250-W mercury lamp, while the same 100% decoloration ratio was achieved after 6 h when BYLAB UV-III UV light desktop with power of 12-W was used at irradiation wavelength of 365 nm under the same reaction condition.

**Table 2** Effect of pH on photocatalytic decolorizing efficiency of 50 ml of 2.0 mg/L RhB solution over 2.0 mg of compound **2**.

Batch	pH	Equilibrium time <sup>[b]</sup> (h)	Decoloration ratio (%)
No.1	6.0	3.5	66.9
No.2	5.0	4.0	92.2
No.3	4.0	3.0	96.1
No.4	3.5	6.0	100.0
No.5 <sup>[a]</sup>	3.5	< 1.25	100.0
No.6	3.0	1.5	85.6

[a] 250-W mercury lamp was used as a light source instead of the BYLAB UV-III UV light desktop with power 12-W and irradiation wavelength 365 nm. [b] Time when the degradation ratio remains unchanged.

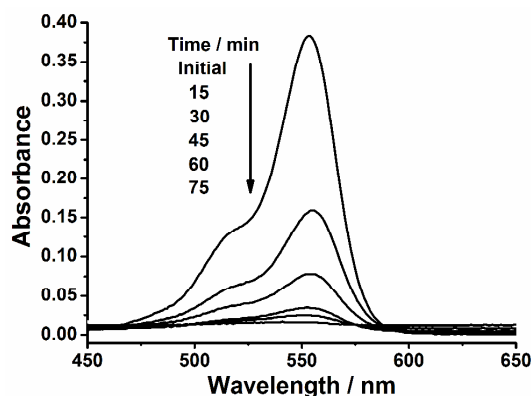


**Fig. 2.** UV-vis absorption spectral changes of RhB during the catalytic process using a 250-W mercury lamp as a light source. The arrow marks the increase of reaction time. Reaction condition: pH 3.5, 2.0 mg of the compound **2**.

Additionally, it was also found that both speed and decoloration ratio of catalysis remarkably enhanced with increasing the dosage of catalyst (0.5 - 3.0 mg) for compound **2** (Figure S5, Table 3) at optimal pH range (3.0 ~ 5.0).

**Table 3** Effect of catalyst dosage of compound **2** on photocatalytic decolorizing efficiency with 50 ml of 2.0 mg/L RhB solution.

Batch	pH	Dosage of Catalyst	Time (h)	Decoloration ratio (%)
No.1	3.5	0.5	6.0	22.0
No.2	3.5	1.0	6.0	50.0
No.3	3.5	1.5	6.0	88.0
No.4	3.5	2.0	6.0	100.0
No.5	3.5	3.0	3.5	99.8
No.6	4.0	1.0	6.0	62.3
No.7	4.0	2.0	6.0	100.0

Initial concentration of RhB also affects the decoloration ratio,



the apparent exponential decay curves were obtained for 0.5 ~ 6 mg/L of the RhB solution when degradation rate was plotted versus time (Figure 3). It exhibits an optimum dye concentration (2.0 mg/L) at pH 3.5 in the presence of 2.0 mg of compound 2.

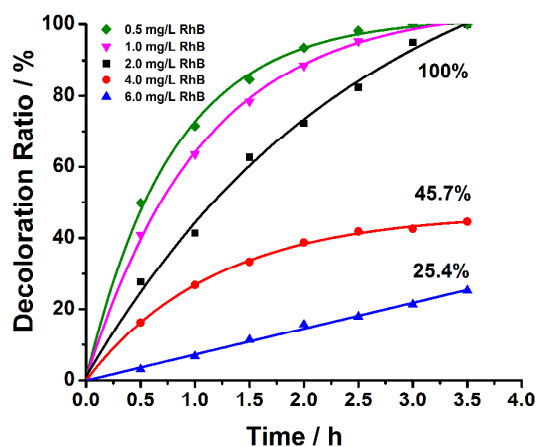


Fig. 3. Effects of RhB concentration (50 ml) under pH 3.5 in the presence of 2.0 mg of compound 2.

up to *ca.* 80 % with long reaction time of 23 h by using 6.0 mg/L concentration of RhB solution. This phenomenon suggests that when initial dye concentration is beyond a threshold, effective light penetration is seriously hindered and competitive absorption starts to inhibit the photochemical formation<sup>20</sup>. In other words, UV light cannot penetrate into the RhB containing solution when the concentration of RhB is too high in it. As a result, only a small percentage of POMs can absorb UV light and leads to the lower decoloration ratio.

The experimental results showed that when compound 1 (quite soluble in water) was added to the RhB solution, the concentration of RhB in solution was notably decreased with the passage of time, which was demonstrated by the decrease of characteristic RhB peak at 554 nm. However, unlike the situation for compound 2, compound 1 was unstable and decomposed simultaneously during catalysis process, which could be recognized from the reduction of the characteristic absorption at 450 nm that is ascribed to the Keplerate type POM anion (Figure 4a).<sup>3-4,7-8</sup> After complete decomposition of compound 1, absorbance intensity of the characteristic RhB peak at 554 nm corresponding to concentration of RhB did not change any more. The similar situation was observed for compound 3. As compared to compound 1, the compound 3 decomposed more easily in water during the catalytic process due to its higher anionic charge, which was revealed by fast disappearance of the characteristic absorption at 450 nm that was ascribed to the Keplerate type POM anion (Figure 4b). By contrasting the situation for compound 1 and 3, the characteristic absorption of compounds 2 and 5 was not found in reaction solution, indicating that they are quite insoluble in water. It can be deduced from results that the {Mo<sub>132</sub>} anions in the compounds are the active centers under UV-irradiation to degrade RhB. However, the water-soluble compounds 1 and 3 were naturally unstable in solution and could be decomposed completely within a certain period of time, this means that the Keplerate type {Mo<sub>132</sub>} anions

need to be stabilized and protected in aqueous solution. In this context, combination of {Mo<sub>132</sub>} anions and *n*-Bu<sub>4</sub>N<sup>+</sup> or DODA<sup>+</sup> results in formation of a new kind of heterogeneous catalysts, viz., compound 2, 4, and 5, where the organic cations endow

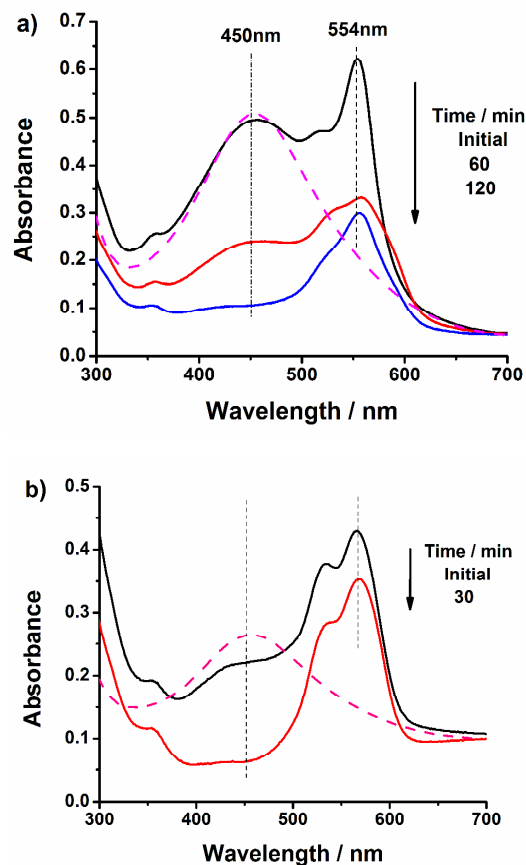


Fig. 4. UV-vis absorption spectral changes of RhB solution during the catalytic process with a) compound 1 and b) compound 3 as catalyst. The dash line represents UV-vis absorption spectra of compound 1 and compound 3, respectively. The arrow marks the increase of reaction time. Reaction condition: 50 ml of 2.0 mg/L RhB solution and pH 3.5.

remarkable stability of anions because of their water-tolerant property and hydrophobic interactions between the alkyl chains of *n*-Bu<sub>4</sub>N<sup>+</sup> or DODA<sup>+</sup> cations in the hybrid materials in solid state as a reported case for the giant wheel system with DODA<sup>+</sup> cations.<sup>21</sup>

Surprisingly, when quite stable compound 5 was used as photocatalyst, the decoloration ratio of RhB was calculated to be *ca.* 21% with quite a long reaction time of 23 h (Figure S6) under the same conditions (50 ml of 2.0 mg/L RhB solution with pH 3.5, 2.0 mg of compound 5). Further, for comparison, commercially available TiO<sub>2</sub> was used instead of the compound 2 to degrade RhB, it was found that the decomposition ratio could reach to *ca.* 76%, which is inferior to compound 2, within 4 h reaction time under the same experimental conditions (Figure S7).

On the other hand, considering that the [Mo<sup>VI</sup><sub>72</sub>Mo<sup>V</sup><sub>60</sub>O<sub>372</sub>(SO<sub>4</sub>)<sub>30</sub>(H<sub>2</sub>O)<sub>72</sub>]<sup>72-</sup> bears (-)72 charges, which is larger than that of [Mo<sup>VI</sup><sub>72</sub>Mo<sup>V</sup><sub>60</sub>O<sub>372</sub>(CH<sub>3</sub>COO)<sub>30</sub>(H<sub>2</sub>O)<sub>72</sub>]<sup>42-</sup>, it is interesting to consider the charge influence on the catalytic activities of their corresponding derivatives. Therefore, compound 4 (a derivative of the compound 3) was tested for RhB

solution decoloration under the same condition (50 ml of 2.0 mg/L RhB solution with pH 3.5, 2.0 mg of compound 4) as that for the compound 2. It was found that when compound 4 was used as a catalyst the characteristic absorption of RhB solution decreased to *ca.* 73% after 17 h stirring under UV light (Figure S8). The adsorption site did not drift as the case for the compound 2. As compared to compound 2, the compound 4 showed weak catalytic activities under the same condition.

Taken the above results into account, it is known that these three heterogenous catalysts showed the following order compound 2 > compound 4 >> compound 5 in view of catalytic effect. The reason for the phenomena can be tentatively explained as follows: in the case of *n*-Bu<sub>4</sub>N<sup>+</sup> as cations for {Mo<sub>132</sub>} anions, each [Mo<sup>VI</sup><sub>72</sub>Mo<sup>V</sup><sub>60</sub>O<sub>372</sub>(SO<sub>4</sub>)<sub>30</sub>(H<sub>2</sub>O)<sub>72</sub>]<sup>72-</sup> anion has potential to combine more *n*-Bu<sub>4</sub>N<sup>+</sup> cations than each [Mo<sup>VI</sup><sub>72</sub>Mo<sup>V</sup><sub>60</sub>O<sub>372</sub>(CH<sub>3</sub>COO)<sub>30</sub>(H<sub>2</sub>O)<sub>72</sub>]<sup>42-</sup> anion because of difference in negative charge numbers, which causes the number of accessible catalytic active centers of compound 4 less than that of compound 2. This may be responsible for the lower catalytic effect of compound 4 because the anions in compounds 2 and 4 are nearly the same except their anionic charges due to different L in the [Mo<sup>VI</sup><sub>72</sub>Mo<sup>V</sup><sub>60</sub>O<sub>372</sub>(L)<sub>30</sub>(H<sub>2</sub>O)<sub>72</sub>]<sup>n-</sup> structures. Though the difference in the number of *n*-Bu<sub>4</sub>N<sup>+</sup> cations in compounds 2 and 4 does not look so big, however decoloration results demonstrate that such small difference can influence the photochemical effect due to the large size of the *n*-Bu<sub>4</sub>N<sup>+</sup>. Therefore, it is thought that the proper amount of *n*-Bu<sub>4</sub>N<sup>+</sup> not only endow remarkable stability due to its hydrophobicity but also allow reactant molecules to access the catalytic centers because of short alkyl chains and small steric hindrance, while excess amount of *n*-Bu<sub>4</sub>N<sup>+</sup> surrounding the anion dissipate the advantage. In the case of compound 5, the anion is encapsulated tightly by amphiphile DODA<sup>+</sup> with straight alkyl chain at the anion surface<sup>8</sup> which causes less approach to the catalytically active centers, so less catalytic effect was found for compound 5.

In summary, based on the above experimental results, it can be concluded that the compound 2 has highest photocatalytic activities among the derivative's family, and the optimal condition for RhB degradation was determined as, 50 ml of 2.0 mg/L RhB solution, pH 3.5 ~ 4.0, dosage of compound 2 2.0 ~ 3.0 mg, and reaction time 3 ~ 6 h.

#### TOC measurement and identification of final products in the decoloration of RhB

The TOC changes in RhB solution during the progress of photodegradation reflected the mineralization degree of the dye. The initial RhB solution contained about 1.85 ppm of TOC. In order to check the adsorption of RhB on the catalysts, the dye solution was stirred in the dark for 0.5 h under following condition: 50 ml of 2.0 mg/L RhB solution with pH 3.5, 2.0 mg of the compounds 2, 4 and 5, respectively. After adsorption of RhB over the three compounds reached an equilibrium, it was found that the TOC values of the bulk solution dropped to *ca.* 1.79 ppm showing that *ca.* 3% of RhB was adsorbed on the catalyst for each case.

The TOC changes of RhB under UV-light irradiation using compound 2 as catalyst are shown in Figure 5. The TOC removal of *ca.* 27.9% (from 1.79 to 1.29 ppm) was achieved after 6 h

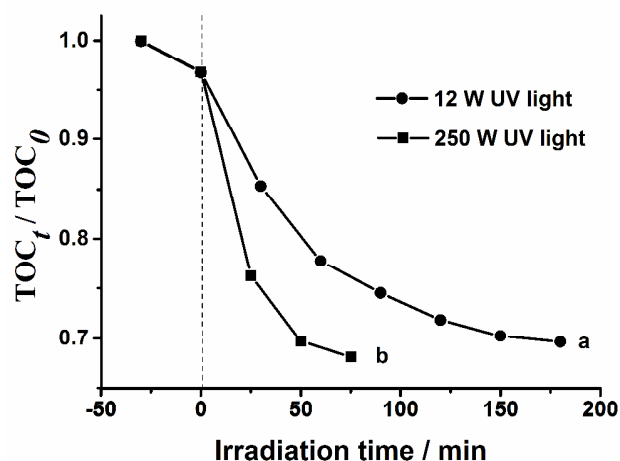


**Fig. 5.** Temporary changes of TOC during photodegradation of RhB (pH 3.5) using compound 2 by a) the BYLAB UV-III UV light desktop with power 12W and irradiation wavelength 365 nm; b) a 250-W high pressure mercury lamp.

stirring when complete decoloration of the dye solution (line a in Figure 5) was finished. The TOC values decreased from 1.79 to 1.40 ppm after 17 h stirring when the compound 4 was used as a catalyst, corresponding to TOC removal of *ca.* 21.8%. While in the case of compound 5 as catalyst, the TOC was removed only by 4.5% (from 1.79 to 1.70 ppm) after 23 h stirring. Notably, when the intensity of UV light was enhanced by using a 250-W mercury lamp (light intensity 22 mW/cm<sup>2</sup>) instead of BYLAB UV-III UV light desktop with power 12 W (light intensity 13 μW/cm<sup>2</sup>), the TOC value dropped from 1.79 to 1.26 ppm, corresponding to 29.6% removal of TOC, within a much shorter time of 75 min (line b in Figure 5) by using the compound 2 as catalyst. These results matched quite well with the photocatalytic decolorizing efficiency of the catalysts obtained from the above UV-vis absorption spectral results.

**Table 4** Predominant products of the photodegradation of RhB and their amount detected by GC/MS using the compound 2 as catalyst.

Retention time (min)	Detected product	Relative product amount
1.42		0.23
1.48		1.00
1.57		0.36
1.64		0.11

It should be noted that color of RhB solution faded gradually upon its decomposition in the presence of the catalysts, and concomitantly, the characteristic absorbance peak of RhB at 554 nm gradually decreased without any peak shift (Figure 1). This observation of no peak shift indicates that the opening of benzene ring was the main process during the catalytic process.<sup>22</sup> Further

the small peaks between 200 nm to 450 nm gradually decreased without peak shift and finally disappeared, indicating that the fragments generated as a result of ring-opening degraded easily during the catalytic process with time.

GC/MS was used to analyze the final products and the corresponding concentrations of RhB degradation. The results (see Table 4) showed that the photodegradation of RhB in the presence of different catalysts under the UV light produced the same products with different concentrations. In this paper, four predominant products were analysed and some other products with less intensities were neglected. These products were mainly come from partially cleaved conjugated xanthene structure of RhB during the degradation reaction. It should be noted that the photodegradation products of RhB produced under different experimental systems may differ from each other, and a direct and simple comparison is not allowed.<sup>23, 24</sup>

### The understanding for the mechanism of catalytic reaction

Generally, it is accepted that under UV irradiation, excitation of POM molecule induces an electronic transition from the highest occupied molecular orbital (HOMO) to the lowest unoccupied molecular orbital (LUMO). The excited state of POM (POM\*) in a water solution can generate  $\cdot\text{OH}$  radicals<sup>25-27</sup> which are extremely powerful oxidizing agents for organic substrates. The reduced POM (POM<sup>-</sup>) produced from the POM\* by abstracting an electron from substrates can deliver the electron to electron acceptors<sup>28-29</sup> such as O<sub>2</sub>, metal ions, and then change into oxidized POM form again. In other words, the hydroxyl free radicals mechanism was commonly involved in POMs-based photocatalysis.

So far no literature has been reported about photocatalytic activities and mechanism for the Keplerate type Mo-O based polyoxometalates. Whether the hydroxyl free radicals were applied for this photocatalytic processes needs to study. As it is known that hydroxyl radicals involved in a photoreaction can be detected by the photoluminescence (PL) technique using terephthalic acid as a probe molecule because the hydroxyl radicals react readily with terephthalic acid to produce highly fluorescent product 2-hydroxyterephthalic acid.<sup>30</sup> The principal of this method is based on the PL signal of 2-hydroxyterephthalic acid at 425 nm. Moreover, the PL intensity of 2-hydroxyterephthalic acid is proportional to the concentration of  $\cdot\text{OH}$  radicals which are produced from POMs catalysis. So, a similar procedure for the measurement of photocatalytic activity was carried out where just the RhB aqueous solution was replaced by aqueous solution of terephthalic acid ( $5 \times 10^{-4}$  M) with NaOH solution ( $2 \times 10^{-3}$  M). A gradual increase in PL intensity at about 425 nm (excited by 315 nm UV-light) was observed with increasing irradiation time for compounds **2**, **4**, and **5** (Figure 6, Figure S9), while no PL increase was observed in the absence of UV light or in the absence of the compounds. This observation indicates that the catalysts indeed produce  $\cdot\text{OH}$  radicals under UV illumination. It was also observed that the PL intensity change was not linear vs the irradiation time, and this can be ascribed to the fact that Mo<sub>132</sub> catalyst is not stable in such high basic condition and Mo<sub>132</sub> catalyst may decompose gradually.

Importantly, under the same condition, the PL intensities were different for the different compounds: the intensity for compound

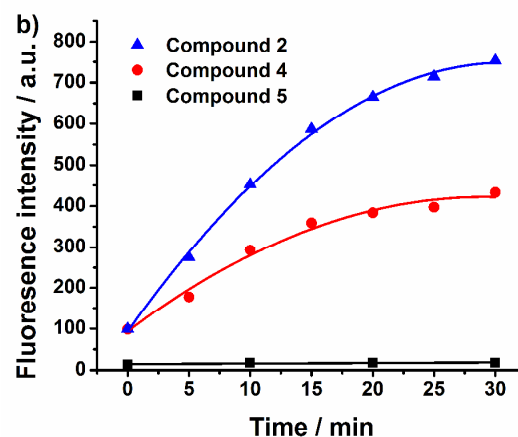
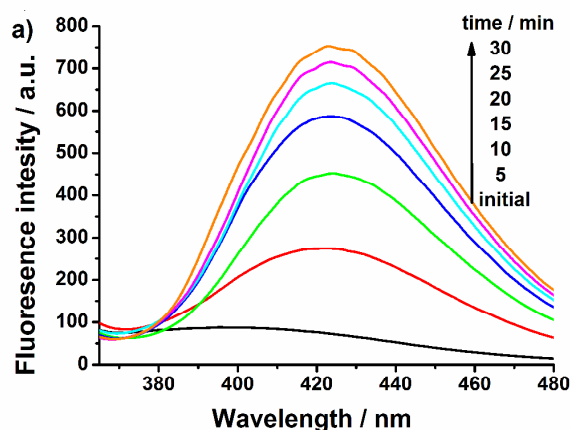


**Fig. 6.** Photoluminescence spectral changes of the compound **2** under UV light irradiation (a), and photoluminescence intensity changes at  $\lambda_{\text{max}} = 425$  nm vs UV light irradiation time of the compound **2**, **4** and **5**. (b) in a  $5 \times 10^{-4}$  M basic solution of terephthalic acid (excitation light  $\lambda = 315$  nm, Voltage = 500V, EX Slit = 10 nm, EM Slit = 10 nm).

**2** > the intensity for compound **4** >> the intensity for compound **5** (Figure 6, Figure S9). This result is quite consistent with their catalytic activities observed above.

In order to get more insight into the possible active species involved during the degradation process in the present study, isopropanol<sup>31</sup> and KI<sup>32</sup> (effective scavengers for  $\cdot\text{OH}$  radicals), benzoquinone<sup>33</sup> (an effective scavenger for O<sub>2</sub><sup>-</sup> radicals) were introduced into the reaction system under the same experimental conditions in separate experiments (Figure 7), respectively. A little effect on the degradation rate of RhB upon addition of benzoquinone into the reaction system was founded, suggesting that the O<sub>2</sub><sup>-</sup> radicals were not the dominant active oxygen species in the present reaction system. Notably, degradation rate of RhB upon addition of either isopropanol or KI into the reaction system decreased greatly, which further confirmed that the  $\cdot\text{OH}$  radicals were the active oxygen species, a result quite consistent with the PL measurement. In addition, it was found that addition of NaN<sub>3</sub><sup>34</sup> (an effective scavenger for both  $\cdot\text{OH}$  radicals and <sup>1</sup>O<sub>2</sub>) led to a remarkable suppression in the photodegradation rate of RhB, indicating that besides  $\cdot\text{OH}$  radicals <sup>1</sup>O<sub>2</sub> also took part in the photo degradation process.

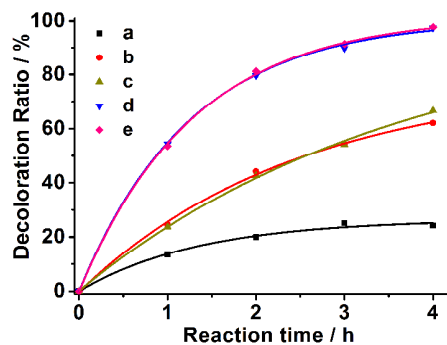


Fig. 7. Plotted degradation kinetics of RhB under UV irradiation on addition of  $\text{NaN}_3$  (a), isopropanol (b), KI (c), benzoquinone (d), and no scavenger added (e). Reaction condition: 50 ml of 2 mg/L RhB solution, 2 mg of compound **2**, 2 mmol/L of scavenger (i.e.,  $\text{NaN}_3$ , isopropanol, KI, benzoquinone).

Taken into account that the Keplerates consist of 12 pentagonal  $\{(\text{Mo}^{\text{VI}})\text{Mo}^{\text{VI}}_5\text{O}_{21}(\text{H}_2\text{O})_6\}$  units and 30 linear  $\{\text{Mo}^{\text{V}}_2\text{O}_4(\text{L})\}$  linker, we believe that the 12 pentagonal  $\{(\text{Mo}^{\text{VI}})\text{Mo}^{\text{VI}}_5\text{O}_{21}(\text{H}_2\text{O})_6\}$  units of Keplerates having  $\text{Mo}^{\text{VI}}$  centers rather than 30 linear  $\{\text{Mo}^{\text{V}}_2\text{O}_4(\text{L})\}$  linkers are the active centers to generate  $\cdot\text{OH}$  radicals, because oxidation state of the Mo species in the  $\{\text{Mo}^{\text{V}}_2\text{O}_4(\text{L})\}$  unit is already (+)5.

#### Separation, stability and recovery of the catalyst

As compound **2** is found the most active one towards the photocatalytic decoloration of RhB solution under the obtained optimal condition, the recovery and reuse of compound **2** was tested. At the completion of photocatalytic reaction, the suspensions were collected by filtration through a polycarbonate film with an average pore diameter of 15 nm, thoroughly washed with water to remove the RhB which was attached on the surface of catalyst. Then the catalyst was reused in the catalytic experiments. The catalytic activity of the recovered compound **2**

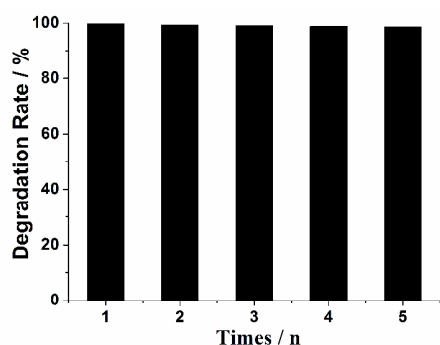


Fig. 8. The catalytic activity of recovered compound **2** versus cycling runs.

for the decoloration of RhB was still satisfactory after 5 repeated experiments (Figure 8). The slight reduction of decoloration ratio was owed to unavoidable lost of the catalyst during repeating regeneration processes. The IR spectra of the catalyst did not show distinct changes after 5 repeated experiments (Figure S10). Decomposition of the compound **2** in solution under catalytic conditions was excluded by performing ICP analysis for Mo in the filtration after complete removal of the suspension at the completion of photocatalytic reaction. These indicate unambiguously that compound **2** remained quite stable and its

structure remained intact under the catalytic condition. Otherwise, the situation as illustrated in Figure 4a would have taken place.

## Conclusions

The photocatalytic activities of a derivative family of the Keplerate type nano-porous Mo-O based polyoxometalates with general formula  $[\text{Mo}^{\text{VI}}_{72}\text{Mo}^{\text{V}}_{60}\text{O}_{372}(\text{L})_{30}(\text{H}_2\text{O})_{72}]^{n-}$  ( $\text{L} = \text{CH}_3\text{COO}^-$ ,  $\text{SO}_4^{2-}$ ) were evaluated first time by a prototype photocatalytic decoloration of RhB solution. The  $\text{Mo}_{132}$  anions were founded to be the active centers under UV irradiation to degrade RhB, while they were unstable in solution and need to be protected by organic cations endowing stability on the anions due to the resultant water-tolerant property and the hydrophobic interactions between the alkyl chains of cations in the hybrid materials in solid state. Analytical mechanism indicates that both  $\cdot\text{OH}$  radicals and  $^1\text{O}_2$  participate in the photo degradation process. The compound **2** showed the highest photocatalytic activity due to the largest formation rate of hydroxyl radicals. It is expected that this study will open a new perspective for the Keplerate type nano-porous Mo-O based polyoxometalates in respect to widely possible applications in photocatalysis which is unexplored yet.

## Acknowledgements

The financial support of the Natural Science Foundation of China, PCSIRT(No. IRT1205) and Beijing Engineering Center for Hierarchical Catalysts is greatly acknowledged. Prof. Xue Duan of Beijing University of Chemical Technology is greatly acknowledged for his kind support.

## Notes and references

State Key Laboratory of Chemical Resource Engineering, Institute of Science, Beijing University of Chemical Technology, Beijing 100029, P.R. China. Fax: +86-10-64414640; Tel: +86-10-64414640; E-mail: zhousy@mail.buct.edu.cn

† Electronic Supplementary Information (ESI) available: [details of any supplementary information available should be included here]. See DOI: 10.1039/b000000x/

‡ Footnotes should appear here. These might include comments relevant to but not central to the matter under discussion, limited experimental and spectral data, and crystallographic data.

- C. L. Hill, *Chem. Rev.*, 1998, **98**, 1-387.
- D. Long, R. Tsunashima, L. Cronin, *Angew. Chem. Int. Ed.*, 2010, **49**, 1736-1758.
- A. Müller, E. Krickemeyer, H. Bögge, M. Schmidtman, F. Peters, *Angew. Chem. Int. Ed.*, 1998, **37**, 3359-3363.
- A. Müller, E. Krickemeyer, H. Bögge, M. Schmidtman, B. Botar, M. O. Talismanova, *Angew. Chem. Int. Ed.*, 2003, **42**, 2085-2090.
- A. Müller, S. K. Das, S. Talismanov, S. Roy, E. Beckmann, H. Bögge, M. Schmidtman, A. Merca, A. Berkle, L. Allouche, Y. Zhou, L. Zhang, *Angew. Chem. Int. Ed.*, 2003, **42**, 5039-5044.
- A. Müller, D. Rehder, E. T. K. Haupt, A. Merca, H. Bögge, M. Schmidtman, G. Heinze-Brückner, *Angew. Chem. Int. Ed.*, 2004, **43**, 4466-4470.
- D. G. Kurth, A. Chesne, D. Volkmer, M. Ruttorf, B. Richer, A. Müller, *Chem. Mater.*, 2000, **12**, 2829-2831.
- D. Volkmer, D. G. Kurth, H. Schnablegger, P. Lehmann, M. J. Koop, A. Müller, *J. Am. Chem. Soc.*, 2000, **122**, 1995-1998.
- P. Kögerler, B. Tsukerblat, A. Müller, *Dalton Trans.*, 2010, **39**, 21-36.
- L. Zhang, Y. Zhou, R. Han, *Eur. J. Inorg. Chem.*, 2010, **17**, 2471-2475.
- C. Schäffer, A. M. Todea, H. Bögge, O. A. Petina, E. T. K. Haupt, A. Müller, *Chem. Eur. J.*, 2011, **17**, 9634-9639.



- 12 S. Garai, E. T. K. Haupt, H. Bögge, A. Merca, A. Müller, *Angew. Chem. Int. Ed.*, 2012, **51**, 10528-10531.
- 13 I. V. Kozhevnikov, *Chem. Rev.*, 1998, **8**, 171-198.
- 14 M. Sadakane, E. Steckhan, *Chem. Rev.*, 1998, **98**, 219-237.
- 5 15 S. Kopilevich, A. Gil, M. Garcia-Ratés, J. B. Avalos, C. Bo, A. Müller, I. A. Weinstock, *J. Am. Chem. Soc.*, 2012, **34**, 13082-13088.
- 16 C. Besson, S. Schmitz, K. M. Capella, S. Kopilevich, I. A. Weinstock, P. Kögerler, *Dalton Trans.*, 2012, **41**, 9852-9854.
- 17 N. V. Izarova, O. A. Kholdeeva, M. N. Sokolov, V. P. Fedin, *Russ. Chem. Bull., Int. Ed.*, 2009, **58**, 134-137.
- 10 18 Y. Zhou, Z. Shi, L. Zhang, S. Hassan and N. Qu, *Appl. Phys. A: Mater. Sci. Process.*, 2013, **113**, 563-568.
- 19 N. Lu, Y. H. Zhao, H. B. Liu, Y. H. Guo, X. Yuan, H. Xu, H. F. Peng, H. W. Qin, *J. Hazard. Mater.*, 2012, **199-120**, 1-8.
- 15 20 I. Arslan-Alaton, *Dyes Pigm.*, 2004, **60**, 167-176.
- 21 S.-i. Noro, R. Tsunashima, Y. Kamiya, K. Uemura, H. Kita, L. Cronin, T. Akutagawa, T. Nakamura, *Angew. Chem. Int. Ed.*, 2009, **48**, 8703-8706.
- 22 T. Shiragami, S. Fukami, Y. J. Waka, S. Yanagida, *J. Phys. Chem.*, 1993, **97**, 12882-12887.
- 20 23 C. Chen, W. Zhao, P. Lei, *Chem. Eur. J.*, 2004, **10**, 1956-1965.
- 24 P. Lei, C. Chen, J. Yang, *Environ. Sci. Technol.*, 2005, **39**, 8466-8474.
- 25 25 E. Androulaki, A. Hiskia, D. Dimotikali, C. Minero, P. Calza, E. Pelizzetti, E. Papaconstantinou, *Environ. Sci. Technol.*, 2000, **34**, 2024-2028.
- 26 A. Mylonas, A. Hiskia, E. Papaconstantinou, *J. Mol. Catal. A: Chem.*, 1996, **114**, 191-200.
- 27 T. Yamase, T. Kurozumi, *J. Chem. Soc., Dalton Trans.*, 1983, **10**, 2205-2209.
- 30 28 A. Troupis, A. Hiskia, E. Papaconstantinou, *New J. Chem.*, 2001, **25**, 361-363.
- 29 A. Troupis, A. Hiskia, E. Papaconstantinou, *Angew. Chem. Int. Ed.*, 2002, **41**, 1911-1914.
- 35 30 J. Yu, G. Dai, B. Cheng, *J. Phys. Chem. C.*, 2010, **114**, 19378-19385.
- 31 G. T. Li, K. H. Wong, X. W. Zhang, C. Hu, J. C. Yu, R. C. Y. Chan, P. K. Wong, *Chemosphere*, 2009, **76**, 1185-1191.
- 32 C. Karunakaran, R. Dhanalakshmi, *Sol. Energy Mater. Sol. Cells.*, 2008, **92**, 1315-1321.
- 40 33 C. Schweitzer, R. Schmidt, *Chem. Rev.*, 2003, **103**, 1685-1757.
- 34 S. Zhao, X. H. Wang, M. X. Huo, *Appl. Catal. B: Environ.*, 2010, **97**, 127-134.

The photocatalytic potential of a derivative family of the unique Keplerate type nanoporous Mo-O based polyoxometalates has been evaluated.

